Appendices

A.1 Dynamic Modeling

We begin our dynamic model with the planar motion of a three degree of freedom brain that is uncoupled from the skull. As seen in the kinematics section, the motion of brain's center of mass is constrained to a single degree of freedom according to the PCA analysis. In the small angle regime, this is indicative of a rolling motion between the brain and skull. Using the kinematic analysis, we determine a center of rotation for the brain, which is defined as the point in the brain that translates minimally in the skull frame. The translational motion of the center of rotation is not completely eliminated, however, there still exists a linear relationship between brain's relative angle and the relative translation. This relationship is represented as a kinematic constraint that reduces the constrained three degree of freedom to a single independent degree of freedom. We chose to use the brain's relative angle as the independent degree of freedom because of the importance of brain rotation in diffuse axonal injury [30, 12].

Below, we furnish the equations of motion that were used in the constrained dynamic model.

Table 3: Glossary of model parameters

Variables	Description
T	Kinetic energy
$\hat{n}_x, \hat{n}_y, \hat{n}_z$	Unit vectors in the reference frame
$\hat{S}_x, \hat{S}_y, \hat{S}_z$	Unit vectors in the skull frame
$\hat{b}_x, \hat{b}_y, \hat{b}_z$	Unit vectors in the brain frame
x_s, z_s	Translation of the skull reference
θ_s	Rotation of the skull reference
x_b, z_b	Relative translation of the brain center of rotation
θ_b	Relative rotation of the brain
d_x, d_z	Position of the brain center of rotation w.r.t. the brain center of mass
k, c	Spring stiffness and damping respectively of the torsional spring
m	Mass of the brain
I	Moment of inertia of the brain about the brain center of mass

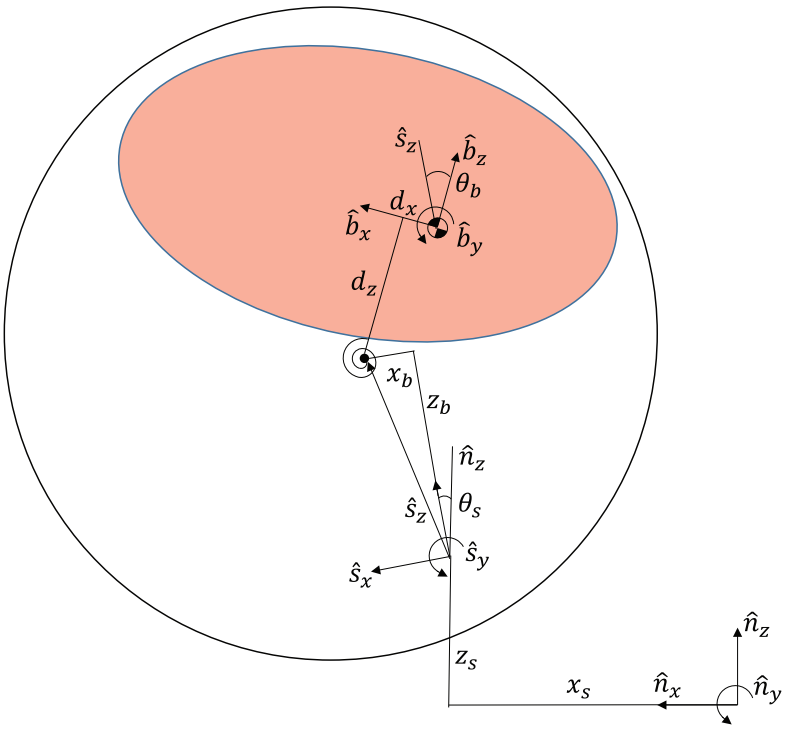

Figure 8: Rigid body diagram of the brain-skull system detailing the parameters and variables. The skull and brain are rigid bodies coupled with a torsional spring. The translation of the torsional spring with respect to the skull is coupled to the relative rotation between the skull and brain.

In Table 3, the skull motion variables x_s, z_s, θ_s are given as system inputs while the system outputs are the resulting brain motion variables x_b, z_b, θ_b. We start by writing the Lagrange equations of motion as follows:

$$\frac{d}{dt}\frac{\partial T}{\partial \dot{q}} - \frac{\partial T}{\partial q} = \mathcal{F}_{\dot{q}} \tag{A.1}$$

where T is the kinetic energy and consists of a rotational and a translational component, q is an arbitrary variable, and the right hand side give the fores that are exerted on the system. Brain's kinetic energy can be written as:

$$T_{rotational} = \frac{1}{2} I \left(\dot{\theta}_s + \dot{\theta}_b\right)^2 \tag{A.2}$$

$$T_{translational} = \frac{1}{2} m \left[\dot{x}_s^2 + \dot{z}_s^2 + \left(\dot{x}_b + z_b \dot{\theta}_s\right)^2 + \dots\right.$$

$$\left(\dot{z}_b - x_b\dot{\theta}_s\right)^2 + \left(\dot{\theta}_s + \dot{\theta}_b\right)^2 (d_x^2 + d_z^2) + \ldots$$
$$2\left(\dot{x}_s cos(\theta_s) - \dot{z}_s sin(\theta_s)\right)\left(\dot{x}_b + z_b\dot{\theta}_s\right) + \ldots$$
$$2\left(\dot{x}_s sin(\theta_s) + \dot{z}_s cos(\theta s)\right)\left(\dot{z}_b - x_b\dot{\theta}_s\right) + \ldots$$
$$2\left(d_x sin(\theta_s + \theta_b) - d_z cos(\theta_s + \theta_b)\right)\dot{x}_s\left(\dot{\theta}_s + \dot{\theta}_b\right) + \ldots$$
$$2\left(d_z sin(\theta_s + \theta_b) + d_x cos(\theta_s + \theta_b)\right)\dot{z}_s\left(\dot{\theta}_s + \dot{\theta}_b\right) + \ldots$$
$$2\left(d_x sin(\theta_b) - d_z cos(\theta_b)\right)\left(\dot{x}_b + z_b\dot{\theta}_s\right)\left(\dot{\theta}_s + \dot{\theta}_b\right) + \ldots$$
$$2\left(d_x cos(\theta_b) + d_z sin(\theta_b)\right)\left(\dot{z}_b - x_b\dot{\theta}_s\right)\left(\dot{\theta}_s + \dot{\theta}_b\right)\Big] \tag{A.3}$$

and the generalized forces as:

$$\mathcal{F}_{\dot{q}} = \left[F_x\hat{s}_x + F_z\hat{s}_z + mg\hat{n}_x\right]\frac{\partial(\dot{x}_b\hat{s}_x + \dot{z}_b\hat{s}_z)}{\partial\dot{q}} + \left[-k\theta_b - c\dot{\theta}_b\right]\frac{\partial(\dot{\theta}_b\hat{s}_y)}{\partial\dot{q}} \tag{A.4}$$

where F_x and F_z are the reaction forces applied to the brain at the center of rotation from the skull, and k and c are stiffness and damping parameters respectively for the torsional spring. Using the Lagrange formulation in Equation 1, the kinetic energy of the brain defined in Equation 1 and the generalized forces acting on the brain in Equation 2, we derive the equations of motion for each generalized coordinate:

- Generalized coordinate: x_b:

$$m\Big[\ddot{x}_b + z_b\ddot{\theta}_s + 2\dot{z}_b\dot{\theta}_s + \ddot{x}_s cos(\theta_s) - \ddot{z}_s sin(\theta_s) - \dot{\theta}_s^2 x_b + \ldots$$
$$(\ddot{\theta}_s + \ddot{\theta}_b)(d_x sin(\theta_b) - d_z cos(\theta_b)) + \ldots$$
$$(\dot{\theta}_b + \dot{\theta}_s)^2(d_x cos(\theta_b) + d_z sin(\theta_b))\Big] = F_x + mgcos(\theta_s) \tag{A.5}$$

- Generalized coordinate: z_b:

$$m\Big[\ddot{z}_b - x_b\ddot{\theta}_s - 2\dot{x}_b\dot{\theta}_s + \ddot{x}_s sin(\theta_s) + \ddot{z}_s cos(\theta_s) - \dot{\theta}_s^2 z_b + \ldots$$
$$(\ddot{\theta}_s + \ddot{\theta}_b)(d_z sin(\theta_b) + d_x cos(\theta_b)) + \ldots$$
$$(\dot{\theta}_s + \dot{\theta}_b)^2(d_z cos(\theta_b) - d_x sin(\theta_b)\Big] = F_z + mgsin(\theta_s) \tag{A.6}$$

- Generalized coordinate: θ_b:

$$\left[I + m(d_x^2 + d_z^2)\right](\ddot{\theta}_s + \ddot{\theta}_b) + \ldots$$
$$m\left[\ddot{x}_s(-d_z cos(\theta_s + \theta_b) + d_x sin(\theta_s + \theta_b)) + \ldots\right.$$
$$\ddot{z}_s(d_x cos(\theta_s + \theta_b) + d_z sin(\theta_s + \theta_b)) + \ldots$$
$$(\ddot{x}_b + z_b\ddot{\theta}_s + \dot{z}_b\dot{\theta}_s)(d_x sin(\theta_b) - d_z cos(\theta_b)) + \ldots$$

$$
\begin{aligned}
(\ddot{z}_b - x_b\ddot{\theta}_s - \dot{x}_b\dot{\theta}_s)(d_x cos(\theta_b) + d_z sin(\theta_b)) + \ldots \\
\dot{\theta}_s(\dot{x}_b + z_b\dot{\theta}_s)(d_z sin(\theta_b) + d_x cos(\theta_b)) + \ldots \\
\dot{\theta}_s)(\dot{z}_b - x_b\dot{\theta}_s)(d_z cos(\theta_b) - d_x sin(\theta_b))\Big] = \ldots \\
-k\theta_b - c\dot{\theta}_b + mgsin(\theta_s)(d_x cos(\theta_b) + d_z sin(\theta_b)) + \ldots \\
mgcos(\theta_s)(d_x sin(\theta_b) - d_z cos(\theta_b))
\end{aligned} \tag{A.7}
$$

To reduce the 3 generalized coordinates to a single independent degree of freedom, we impose two kinematic constraints:

$$
\{\, x_{\,b} = \alpha\theta_b z_b = \beta\theta_b \tag{A.8}
$$

It should be noted that the fitted values for the distance between brain's center of mass and center of rotation, fitted to the MRI measurement of brain motion, were determined as $dx = 0.011,\ -0.005,\ 0.006m$ and $dz = -0.038,\ -0.045,\ -0.041m$ for the three subjects, respectively.

A.2 Frequency Modeling

We begin our frequency analysis by reducing our constrained dynamic model to a Single-Input Single-Output (**SISO**) model, which parametrizes the relative rotation of the brain with respect to the skull. The translational degrees of freedom of the skull and the brain are decoupled from the relative brain rotation. The justification of the SISO model is based on the strong dependence of the brain rotation on the skull's rotational acceleration. The transmissibility function is defined as the ratio of the output, i.e. the relative brain rotation θ_b, to the input, i.e., skull's rotational acceleration $\ddot{\theta}_s$ in the frequency domain. The inertial parameter (C) is fixed based on the results from the dynamical model. The stiffness and damping parameters are optimized in the frequency domain by using a least-squares approach based on the mismatch between the empirical (i.e., from MRI data) and analytical (i.e., Equation 10) transmissibility amplitudes. All 3 subjects were considered simultaneously for the least-squares optimization and parameter fits. The confidence bound of the frequency domain fit, which turned out to be insignificant when compared with the uncertainty due to the time length of experimental measurements is computed by using the confidence intervals of stiffness and damping parameters.

We linearized and simplified Equation 7, with the following assuming $d_z \gg d_x, \ddot{x}_s \gg \ddot{z}_s$. Furthermore, similar PCA analysis results as discussed in the previous sections hold between the skull accelerations for different DOFs, such that

$$
\ddot{\theta}_s = C\ddot{x}_s \tag{A.9}
$$

where C has an average value of $4.1m^{-1}$ for MRI experiments and -5.8m^{-1} for PMHS experiments. The reason for the negative sign in the PMHS experiment is the fact that the cadaver head was held upside down in those experiments.

Using Equations 5 and 6, and linearizing Equation 7 we obtain

$$I_{CoR}\ddot{\theta}_b + c\dot{\theta}_b + k\theta_b = (Cmd_z - I_{CoR})\ddot{\theta}_s \tag{A.10}$$

where I_{CoR} is the equivalent inertia around the CoR, x_b is the relative rotation of the brain wrt skull and $\ddot{\theta}_s$ is the rotational skull acceleration.

The resulting transmissibility function is derived as:

$$T(\omega) = C\frac{\theta_b(\omega)}{\ddot{\theta}_s(\omega)} = \frac{\frac{Cmd_z}{I_{CoR}} - 1}{(\sqrt{\omega^2 - \omega_n^2})^2 + (2\zeta\omega\omega_n)^2} \tag{A.11}$$

where ω_n is the resonance frequency, ζ is the damping ratio, and ω is the frequency of the input to the system (skull motion).

A.3 Model Verification with PMHS Measurements

In this section, we verify the 1DOF dynamic model both in frequency and time domains with brain displacement data derived from x-ray measurements during PMHS head impacts [17]. This step is crucial to examine the applicability of our model to loadings that are more representative of typical head impacts on the field. We used the neutral density target (**NDT**) displacement data from a test performed in the sagittal plane (protocol C755-T2). In this experiment, the maximum achieved linear and rotational accelerations were $20g$ and $2000rad/s^2$.

First, we compared the frequency response in the PMHS study with the predictions from our 1DOF model. A similar procedure to MRI data analysis was repeated for the PMHS data, where we fitted a 3DOF rigid-body motion to the NDT displacement data [49], and then analyzed the kinematics of the derived rigid-body motion, which showed a different center of rotation and translation path from the MRI data (Figure 5A). Subsequently, we used skull's acceleration and brain's rigid-body rotation as input and output to the transmissibility function (Supplementary Equation 11) and observed that the PMHS data show similar resonating behavior as previously seen in the MRI data (Figure 5B).The predictions from the 1DOF dynamic model with parameters derived from time and frequency domains, as described in the previous section, showed good agreement with the PMHS experimental results.

We also verified the performance of the 1DOF dynamic model in the time domain. Using, the 1DOF dynamic model developed in the previous section and PMHS skull kinematics, we simulated PMHS brain's motion. Similar to error analysis in the previous sections, a histogram of distance errors (for all NDT displacement values and throughout the temporal measurements) between x-ray measurements and model predictions is shown in Figure 9A.

Finally, as an additional step in verifying model accuracy, we compared the 1DOF dynamic model's predictions against a finite element simulation. We used the Simulated Injury Monitor (SIMon), a detailed finite element (FE) brain model developed by the U.S. National Highway Traffic and Safety Administration, that includes detailed geometry and anatomy of brain and skull with more than 30,000 elements [39]. This model has been validated against

brain displacement measurements from the same PMHS experimental protocol in various planes of impact. Interestingly, the 1DOF dynamic model gave similar distance error levels as SIMon for all NDTs for throughout the experimental measurement (Figure 9B). As reference, a representative NDT displacement in IS and PA directions is shown for both 1DOF dynamic model and SIMon (Figure 9C-D).

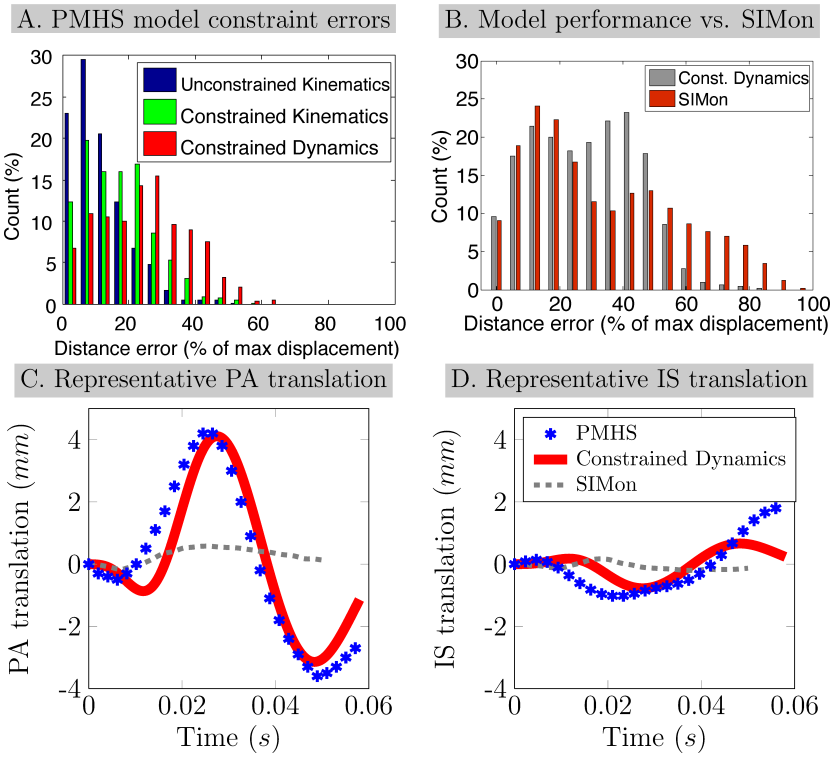

Figure 9: Model consistency verification with cadaver impact experiments: (A) histogram of distance error between the rigid-body model and all the cadaver NDT and comparison of error with SIMon, (B) histogram of distance erros from NDT measurements for the 1DOF dynamic model and SIMon, (C-D) comparison of IS and PA translations predicted with the 3DOF dynamical model versus the cadaver experimental results and SIMon prediction.